Wall-Catalytic Fluorine Recombination in an HF Laser Nozzle

E. J. Jumper*
Air Force Institute of Technology, Wright-Patterson Air Force Base, Ohio
R. G. Wilkins†
Wright-Patterson Air Force Base, Ohio
and
B. L. Preppernau‡
Air Force Wright Aeronautical Laboratories, Wright-Patterson Air Force Base, Ohio

This paper discusses the adaptation of the detailed fluorine wall-recombination model into the fluid-dynamic equations governing the flow of dilute atomic fluorine in a tiny generic-type nozzle reminiscent to those found in HF (and DF) lasers. The wall-recombination model is briefly described, as are the fluid-dynamic equations making up the computational framework within which this study was made. Results are given for a range of nozzle wall temperatures form 450 to 650 K. These results are compared to those obtained when a noncatalytic wall and a fully catalytic wall are assumed.

Nomenclature

$\bar{c}$ = average kinetic speed
c_a = number of surface sites per unit area
c_p = specific heat at constant pressure
D = chemisorption well depth
D_2 = deuterium
DF* = vibrationally excited deuteriumfluoride
$\mathfrak{D}_i$ = diffusivity of species i into the mixture
$\mathfrak{D}_{ij}$ = bimolecular diffusivity of species i into species j
F = atomic fluorine
F_2 = diatomic fluorine
h = Planck constant
h_i = enthalpy of species i
H_2 = hydrogen
HF* = vibrationally excited hydrogenfluoride
k = Boltzmann constant
k_b = backward rate constant
k_f = forward rate constant
K_C = equilibrium constant for molar concentration
K_p = equilibrium constant for partial pressure
k_t = thermal conductivity
m_F = mass of an F atom
M = any atom/molecule
$\mathfrak{M}$ = molecular weight
n = number density
$\dot{n}$ = rate of creation/depletion
$\dot{N}$ = kinetic rate of impingement
p = pressure
q_{recomb} = additional heat transfer to wall due to recombination
$\tilde{R}$ = universal gas constant
S_o = sticking coefficient
S_t = steric factor
T = temperature
u = x component of velocity
v = y component of velocity
W = mass fraction
$\dot{W}$ = mass fraction rate of production
x = position along wall
y = position normal to wall
γ = recombination coefficient
δ = thermal desorption rate
ΔY = distance of cell 1 normal to wall
θ_F = fractional surface coverage for F
θ_{F_2} = fractional surface coverage for F_2
$(\theta_F)_o$ = isolated fractional surface concentration for F
$(\theta_{F_2})_o$ = isolated fractional surface concentration for F_2
ν_R = catalytic recombination rate
μ = viscosity
ρ = density
ϕ_{ij} = defined in Eq. (22)
χ = mole fraction
ψ = compressible stream function

Subscripts

F = atomic fluorine
F_2 = diatomic fluorine
i = species i
j = species j
o = isolated

I. Introduction

THE operation of a chemical laser depends on a population inversion produced in the course of an exothermic chemical reaction.[1] In the case of HF and DF lasers, atomic fluorine is required to react with either H_2 and D_2 to form excited HF* or DF*. This atomic fluorine is often furnished to the mixing/lasing cavity via extremely small (exit-plane half-heights of less than 0.1 cm) supersonic nozzles, referred to as the primary nozzles. It is now known that fluorine will catalytically recombine on surfaces made of materials used in the construction of these nozzles.[2] Such recombination is detrimental to the performance of HF and DF lasers in two ways. The most obvious performance effect is that the amount of F available to form excited species is reduced in direct pro-

Received May 20, 1985; Presented as Paper 85-1598 at the AIAA 18th Fluid Dynamics, Plasmadynamics and Lasers Conference, Cincinnati, OH, July 16–18, 1985; revision received May 13, 1987.

*Professor, Department of Aeronautics and Astronautics. Associate Fellow AIAA.
†Aeronautical Engineer.
‡Research Physicist, Power Division, Propulsion Laboratory.

portion to the amount of F removed by the catalytic recombination. The second effect is less obvious but even more damaging; it has to do with the location of recombinative depletion of F. Since the laser operates via mixing, the atomic fluorine nozzles alternate with H_2 (or D_2) secondary nozzles. As such, the mixing takes place at the shear boundaries. Because the F depletion takes place at the nozzle wall, the atomic fluorine concentration in the immediate vicinity of a shear boundary contains a much lower F concentration than the nozzle flow as a whole. Thus, the formation of the excited species is not only decreased overall, but the excitation reaction tends to be slowed by diffusion times, thereby spreading out the reaction in the cavity along the flow axis.

Unfortunately, the measurement of actual atomic fluorine concentrations at the exit plane of the primary nozzles poses some difficulties (see, for example, Refs. 3 through 6). Further, experimental data for fluorine catalytic recombination are both sparse and configuration-dependent.[2,7] Thus, the acceptance that catalytic recombination has been an important contributor to lower experimental gain realizations than had been theoretically predicted if we assume no catalytic recombination is, for the most part, based on compatibility arguments.

One of the first, and still one of the most graphic examples of these type of compatibility arguments, is found in the work of Mikatarian et al.,[8] in which linear species profiles were used that assumed all the atomic fluorine had been catalytically removed from the flow at the wall and redeposited as molecular fluorine by the time the flow had arrived at the exit plane of the nozzle. The linear species profiles were arbitrarily chosen, but were based on the notion that since the nozzle flow was known to be "fully viscous" (that is, the exit-plane velocity profile was nearly parabolic), a catalytic boundary condition assumed to remove all the atomic fluorine from the flow at the wall would form a full species profile; the linear distributions were assumed to crudely approximate such profiles. These species profiles were then used as initial conditions for the computation of mixing and lasing in the cavity of an HF chemical laser for which experimental data were available. The results of this study clearly demonstrated the spreading out of the reaction along the flow axis, closely matching the experiment. Although the extent of the atomic fluorine depletion by a catalytic wall was only hypothesized, these results gave compelling reasons to suspect that catalytic effects were not only present, but perhaps the most important contributor to the large discrepancies between predicted and experimentally realized gain measurements.

The Mikatarian et al.[8] results prompted a study by Ferrell et al.[9] that attempted to answer the question of whether or not even a "fully catalytic" wall could produce the dramatic profiles suggested by the cavity study of Ref. 8. The Ferrell et al. study demonstrated that such profiles were possible, at least with the assumption that the walls could be treated as fully catalytic. The assumption of a fully catalytic wall was made because at the time of the study,[9] a more realistic model was not available; this is no longer the case.[2]

II. Heterogeneous Chemistry

A "realistic" wall-catalytic (that is, heterogeneous) fluorine recombination model is presented and discussed in detail in Ref. 2 in which the Langmuir-Rideal mechanism[10-13] was successfully applied for a nickel surface. By solving the kinetic rate equations at steady state, and for the temperatures of interest here, the fractional surface converage for atomic fluorine θ_F can be shown to be[2]

$$\theta_F = (\theta_F)_o \frac{1-(\theta_{F_2})_o}{1-(\theta_F)_o(\theta_{F_2})_o} \tag{1}$$

where the so-called isolated fractional surface concentrations $(\theta_F)_o$ and $(\theta_{F_2})_o$ are given by

$$(\theta_F)_o = 1\Big/\left(1+\frac{\delta_F}{S_{o_F}\dot{N}_F}+\frac{S_t}{S_{o_F}}\right) \tag{2}$$

and

$$(\theta_{F_2})_o = 1\Big/\left(1+\frac{\delta_{F_2}}{S_{o_{F_2}}\dot{N}_{F_2}}\right) \tag{3}$$

In Eqs. (2) and (3), δ is the thermal desorption rate[14] and $\dot{N}$ is the kinetic rate of impingement,[15] given, respectively, by

$$\delta = c_a \frac{kT}{h} \exp\ (-D/kT) \tag{4}$$

where c_a is the number of surface sites per unit area, k the Boltzmann constant, h the Planck constant, D the chemisorption well depth (for F or F_2 as applicable), and T the absolute temperature; and

$$\dot{N} = n\frac{\bar{c}}{4} \tag{5}$$

where n is the number density of particles (F or F_2) and $\bar{c}$ the average kinetic speed of the particles at the wall temperature. Also included in Eqs. (2) and (3) are the clean-surface sticking coefficient S_o for F or F_2 as applicable, the functional form of which was taken from Ref. 2, and the steric factor S_t.

The catalytic recombination rate ν_R may be obtained from Eq. (1) as

$$\nu_R = S_t \dot{N}_F \theta_F \tag{6}$$

Since the recombination coefficient γ is defined as two times the ratio of the number of fluorine atom wall collisions resulting in a recombination to the total number of fluorine atom wall collisions, it is given by

$$\gamma = \frac{2\nu_R}{\dot{N}_F} = 2S_t\theta_F \tag{7}$$

The computation of γ via Eqs. (1-7) is relatively simple; however, the resulting solution (using the values of the various parameters shown in Table 1 taken from Ref. 2) is rich in diversity as can be seen in Fig. 1, which represents only one possible concentration distribution; each new variation in concentration would lead to different results. It is, therefore, easier to use Eqs. (1-7) to arrive at γ as a function of the temperature, pressure, and concentration of F and F_2 than to attempt to curve fit the results as functions of these parameters. Such richness of the solution helps to explain the wide variation in reported recombination data where conditions vary from one experiment to another,[16,17] and only underscores the need for the detailed treatement of the problem as proposed in Ref. 2.

III. Homogeneous Chemistry

The only gas-phase (homogeneous) recombination/dissociation reaction of interest in the study was that

Table 1 Physiochemcial parameters

c_a (k/h)	3.388×10^{25} particles/(K s cm^2)
S_t	0.018
D_F	1.261×10^{-12} erg/atom
D_{F_2}	*1.215×10^{-12} erg/molecule*

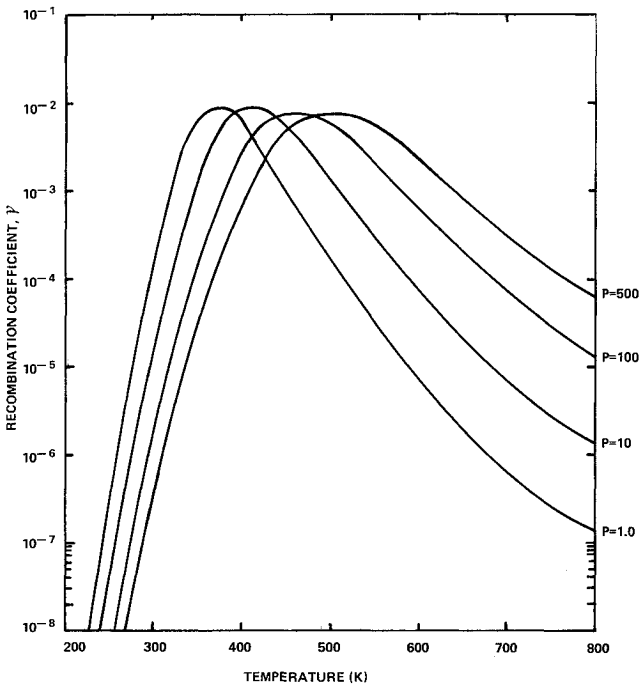

Fig. 1 Plots of calculated values of γ vs temperature from the model of Ref. 2. The curves are for different total pressures (in Torr) for a gas composition by mole fraction of 0.039 F, 0.081 F_2, and 0.88 Ar.

for fluorine. This reaction is given by

$$2F + M \underset{k_b}{\overset{k_f}{\rightleftharpoons}} F_2 + M \tag{8}$$

where M is any other atom/molecule, k_f the forward rate constant, and k_b the backward rate constant. The forward rate constant used was taken from Ref. 8 and is

$$k_f = \frac{4.716 \times 10^{15} e^{(1250/\tilde{R}T)}}{T} \tag{9}$$

where $\tilde{R}$ is the universal gas constant (1.986 Cal/g-mole K), and the units of k_f are cm^6 g-$moles^{-2}$ s^{-1}. The temperature dependence of the backward rate was taken to be

$$k_b = 1.990 \times 10^{13} e^{-(33{,}000/\tilde{R}T)} \tag{10}$$

so that the equilibrium constant for partial pressures of the reaction

$$\tfrac{1}{2}F_2 \rightleftharpoons F \tag{11}$$

was made to match that in the JANAF[18] tables almost exactly over the temperature range from 600 to 2000 K, where the equilibrium constant for partial pressure, K_{p11}, is related to that for molar concentration for the reaction of Eq. (11), K_{C11}, according to the relation

$$K_{p_{11}} = K_{C_{11}} [(82.05)(T)]^{1/2} \tag{12}$$

The constant in Eq. (12) is the universal gas constant in units of cm^3 atm g-$mole^{-1}$ K^{-1}, and the subscript 11 refers to the reaction of Eq. (11). Finally, the equilibrium coefficient of Eq. (8) is related to that for Eq. (11) by

$$K_{p_8} = \left(\frac{1}{K_{p_{11}}}\right)^2 \tag{13}$$

The rate constants, Eqs. (9) and (10), were then used to compute the rate of species creation/depletion via

$$(\dot{n}_{F_2})_M = k_f \rho^3 \frac{W_F^2}{\mathfrak{M}_F^2} \frac{W_M}{\mathfrak{M}_M} - k_b \rho^2 \frac{W_{F_2}}{\mathfrak{M}_{F_2}} \frac{W_M}{\mathfrak{M}_M} \tag{14}$$

where $(\dot{n}_{F_2})_M$ is the rate of creation/depletion of species F_2 in moles/cm^3 s due to collisions with species M; ρ is the density; W_F is the mass fraction of species F; W_{F_2} is the mass fraction of species F_2; W_M is the mass fraction of species M; and $\mathfrak{M}_F$, $\mathfrak{M}_{F_2}$, and $\mathfrak{M}_M$ are the molecular weights of species F, F_2, and M, respectivley. M is any species present so that

$$\dot{n}_{F_2} = \sum_{\text{all } M} (\dot{n}_{F_2})_M \tag{15}$$

Finally, the rate of creation/depletion of F is related to that of F_2 according to the relation

$$\dot{n}_F = -2\dot{n}_{F_2} \tag{16}$$

IV. Fluid Mechanics

Flow Equations

In order to demonstrate the effect of wall recombinations on the flow composition and character in a generic two-dimensional, steady-state, chemical-laser-type nozzle, the nozzle flow was approximated by solving the equations expressing the flux-divergent notions of continuity, momentum, species, and energy cast in boundary-layer form.[19,20] In order to expedite the numerical integration of these equations, they were transformed from x-y space to x-ψ space by the use of the von Mises transformation,[19,21] in which ψ is the compressible stream function given by

$$\frac{\partial \psi}{\partial y} = \rho u; \qquad \frac{\partial \psi}{\partial x} = -\rho v \tag{17}$$

where u and v are the x and y components of velocity. The transformed equations are thus given by

$$\frac{\partial u}{\partial x} = -\frac{1}{\rho u}\frac{dp}{dx} + \frac{\partial}{\partial \psi}\left(\mu \rho u \frac{\partial u}{\partial \psi}\right) \tag{18}$$

$$\frac{\partial W_j}{\partial x} = \frac{\rho}{\rho u}\dot{W}_j + \frac{\partial}{\partial \psi}\left(\rho \mathfrak{D}_j \rho u \frac{\partial W_j}{\partial \psi}\right) \tag{19}$$

$$\frac{\partial T}{\partial x} = \frac{1}{\rho c_p}\frac{dp}{dx} + \frac{\mu \rho u}{c_p}\left(\frac{\partial u}{\partial \psi}\right)^2 - \frac{1}{\rho u c_p}\sum_i \rho \dot{W}_i h_i + \frac{1}{c_p}\left(\sum_i \rho \mathfrak{D}_i \rho u \frac{\partial W_i}{\partial \psi}\frac{\partial h_i}{\partial \psi}\right) + \frac{1}{c_p}\frac{\partial}{\partial \psi}\left(k_t \rho u \frac{\partial T}{\partial \psi}\right) \tag{20}$$

where p is the pressure, μ the viscosity, W_j the mass fraction of species j, $\dot{W}_j$ the mass-fraction rate of production of species j, $\mathfrak{D}_j$ the diffusivity of species j into the mixture, c_p the specific heat at constant pressure, T the temperature, h_j the enthalpy of species j, and k_t the thermal conductivity.

Thermodynamic and Transport Properties

The enthalpy and specific heats for each species, h_i and c_{p_i}, respectively, were calculated in polynomial form in temperature after Ref. 21, and the specific heat of the mixture was obtained as a mass-fraction weighted sum. The

viscosity of each species μ_i was calculated after Ref. 22, and the viscosity of the mixture was then computed by

$$\mu = \sum_{i=1}^{N} \left[(\chi_i \mu_i) \Big/ \left(\sum_{j=1}^{N} \chi_j \phi_{ij} \right) \right] \tag{21}$$

where χ_i is the mole fraction of species i and

$$\phi_{ij} = \frac{1}{\sqrt{8}} \left(1 + \frac{\mathfrak{M}_i}{\mathfrak{M}_j} \right)^{-1/2} \left[1 + \left(\frac{\mu_i}{\mu_j} \right)^{1/2} \left(\frac{\mathfrak{M}_j}{\mathfrak{M}_i} \right)^{1/4} \right]^2 \tag{22}$$

The thermal conductivity was calculated using the Eucken approximation[22] as

$$k_{t_i} = \left(c_{p_i} + \frac{5}{4} \frac{\tilde{R}}{\mathfrak{M}_i} \right) \mu_i \tag{23}$$

and

$$k_t = \sum_{i=1}^{N} \left[(\chi_i k_{t_i}) \Big/ \left(\sum_{j=1}^{N} \chi_j \phi_{ij} \right) \right] \tag{24}$$

The bimolecular diffusivity of species i into species j, $\mathfrak{D}_{ij}$, was calculated after Ref. 22, and these were used to approximate the diffusivity of species i into the mixture as

$$\mathfrak{D}_i = \left[(1 - \chi_i) \Big/ \left(\sum_{\substack{j=1 \\ j \neq i}}^{N} \frac{\chi_i}{\mathfrak{D}_{ij}} \right) \right] \tag{25}$$

Boundary Conditions

The standard boundary conditions for velocity and constant-temperature wall were used. Temperature-gradient-type heat transfer to the wall was then computed using Fourier's heat law. The catalytic-wall boundary conditions are discussed in the next section along with the enhanced heat transfer due to the catalytic-wall reaction.

V. Catalytic-Wall Boundary Conditions

Recombination

Once the recombination coefficient γ is known, either set or determined according to Eqs. (1-7), the boundary condition of species at the wall becomes a gradient-type boundary condition. At the wall, the rate of diffusion of atomic fluorine toward the wall must just equal the rate at which atomic fluorine disappears by catalytic recombination to form diatomic fluorine. In turn, the rate at which diatomic fluorine is formed dictates the rate at which it diffuses away from the wall. This places the following requirements on the mass-fraction gradients

$$\left(\frac{\partial W_F}{\partial y} \right)_{y=o} = \frac{\gamma W_F}{\mathfrak{D}_F} \left(\frac{kT}{2\pi m_F} \right)^{1/2} \tag{26}$$

and

$$\left(\frac{\partial W_{F_2}}{\partial y} \right)_{y=o} = -\frac{\gamma W_F}{2\mathfrak{D}_{F_2}} \left(\frac{kT}{2\pi m_F} \right)^{1/2} \tag{27}$$

where m_F is the mass of a single fluorine atom. The gradient conditions on W_F and W_{F_2} of Eqs. (26) and (27) can be easily adapted to numerical schemes by approximating the gradient as a simple difference and solving for the mass fraction at the wall cell, $W_F(0)$, based on the mass fractions at the first cell out from the wall, $W_F(1)$, a distance ΔY, as

$$W_F(0) = \left\{ (\mathfrak{D}_F W_F(1)) \Big/ \left[\mathfrak{D}_F + \gamma \left(\frac{kT}{2\pi m_F} \right)^{1/2} \Delta Y \right] \right\} \tag{28}$$

and knowing $W_F(0)$, we can determine $W_{F_2}(0)$ as

$$W_{F_2}(0) = W_{F_2}(1) + \frac{W_F(0)}{\mathfrak{D}_{F_2}} \Delta Y \frac{\gamma}{2} \left(\frac{kT}{2\pi m_F} \right)^{1/2} \tag{29}$$

Catalytic-Wall Enhanced Heat Transfer

As discussed in conjunction with Eqs. (26) and (27), there is a net mass flow of atomic fluorine toward the wall and a net mass flow of molecular fluorine away from the wall. If we assume that the wall acts as an inelastic third body, the net difference in diffusively convected enthalpy to and from the wall ends up residing in the wall as thermal energy, and thus enhances the normal temperature-gradient-type heat transfer. Following this reasoning, one arrives at the follow-

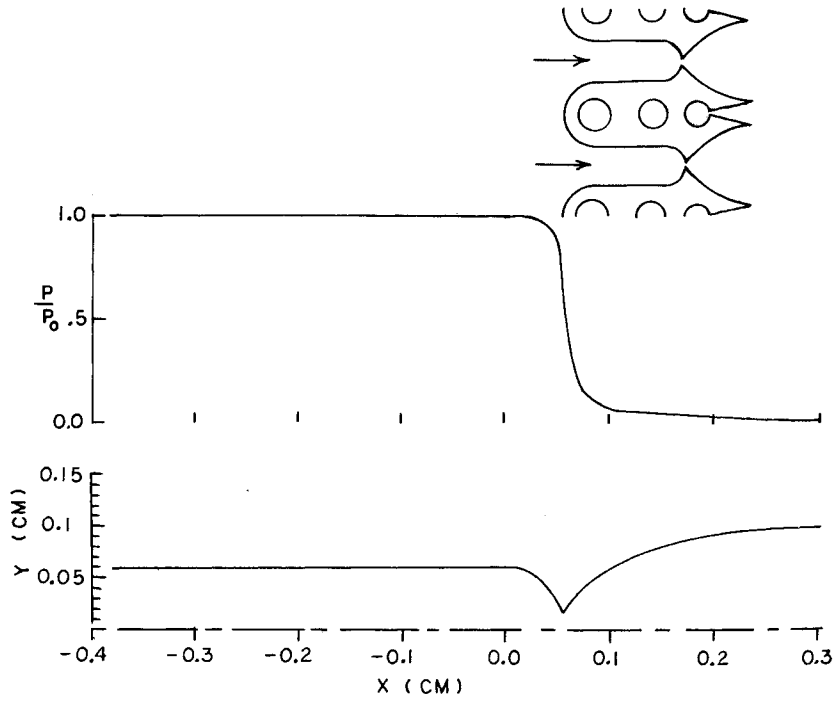

Fig. 2 Pressure distribution as a function of axial position and resulting nozzle shape. Insert indicates a more realistic nozzle geometry for which the profile is an approximation.

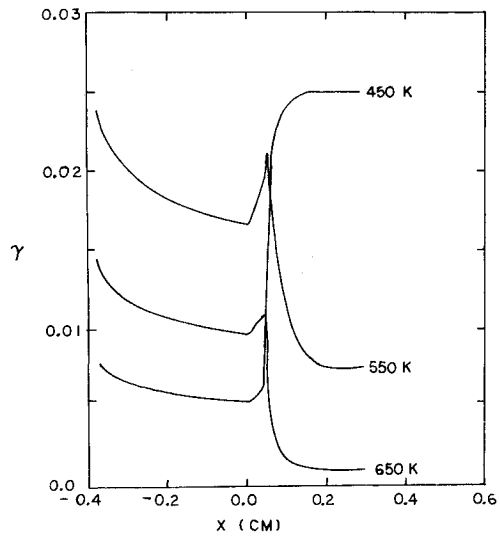

Fig. 3 The recombination coefficient γ, predicted by the model of Ref. 2 as a function of axial position for the nozzle inlet conditions given in Table 2 and for wall temperatures of 450, 550, and 650 K.

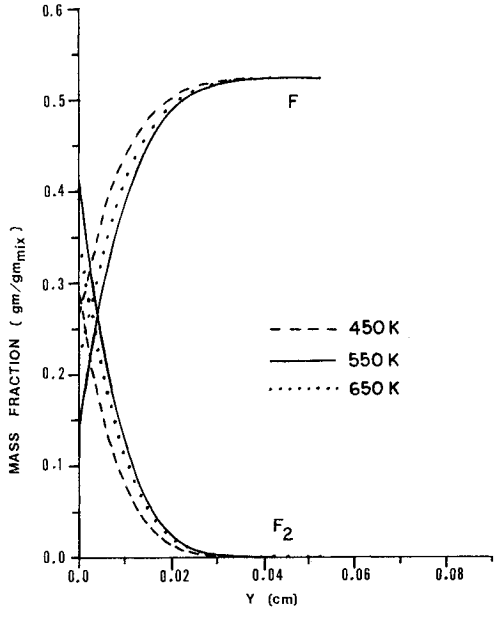

Fig. 4 Species profiles resulting from the use of the model of Ref. 2 for wall temperatures of 450, 550, 650 K, at a location approximately half-way down the subsonic section.

ing formulation of the heat-transfer enhancement per unit area:

$$q_{\text{recomb}} = \rho\gamma W_F(0)\left(\frac{kT}{2\pi m_F}\right)^{1/2}(h_F - h_{F_2}) \qquad (30)$$

where the enthalpies h_F and h_{F_2} are taken to be on a per-mass basis.

VI. Results and Discussion

In order to demonstrate the use of the wall-recombination model on flow in a generic-type laser nozzle, the equations in Section IV were solved numerically (for details of the difference scheme, see Ref. 23) for the pressure profile and subsequent nozzle shape given in Fig. 2. The insert in Fig. 2 shows the type of nozzle configuration being simulated, the long subsonic inlet being required to provide room for the cooling ducts. The cases presented here were run with slug inlet conditions in velocity, temperature, and species as given in Table 2. The results for two series of runs are given.

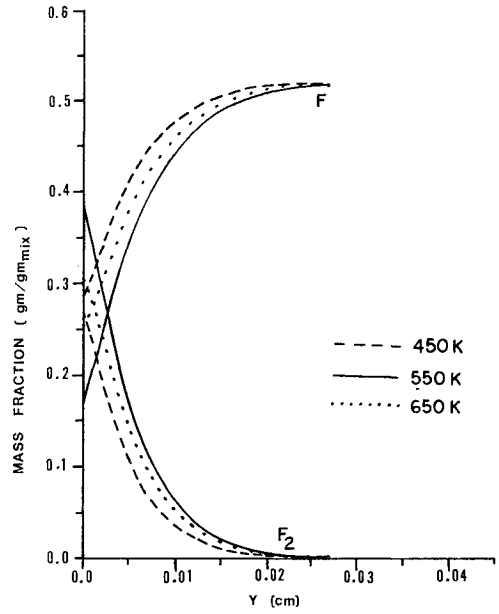

Fig. 5 Same as Fig. 4, but at a location just downstream of the throat.

Table 2 Start-up conditions[a]

Mole fraction of F	0.272
Mole fraction of F_2	0.00035
Inlet velocity	34,000 cm/s
Inlet gas temperature	2000K
Inlet pressure	760 Torr

[a]After Ref. 9.

In the first series, Figs. 3-8, the wall-recombination model described earlier was used to examine the effect of changing wall temperature on recombination coefficient, species, and heat transfer. The range of temperature chosen is of interest for two reasons: First, this range brackets the wall temperatures normally experienced in laser nozzles; and second, it can be seen from Fig. 3 that this range represents those wall temperatures at which γ is first increasing with temperature, goes through a maximum, and then begins to decrease with temperature. This later statement may not seem immediately obvious, because for a wall temperature of 450 K, γ is first less than that for 550 K in the subsonic region and then greater than that for 550 K in the supersonic region. The overall effect, however, is clearly increasing with temperature from a wall temperature of 450 K as can be seen in Figs. 4-7. In the first of these, Figs. 4-6, the net atomic fluorine in the flow is least at a wall temperature of 550 K (in fact, the minimum appears to be closer to 500 than 550 K, the 500 K case will be next addressed). It is apparent from Fig. 6, however, that atomic fluorine is being recombined more rapidly in the supersonic portion of the nozzle at a wall temperature of 450 K than at 550 K, in agreement with Fig. 3. Figure 7 shows that such higher recombination coefficients in the supersonic portion of the nozzle have little overall effect since most of the atomic fluorine is recombined in the subsonic portion of the nozzle.

Figure 8 shows the increased heat transfer due to wall recombination, as discussed in conjunction with Eq. (30). It can be seen that the recombination increases the heat transfer by about a third again over the usual temperature-

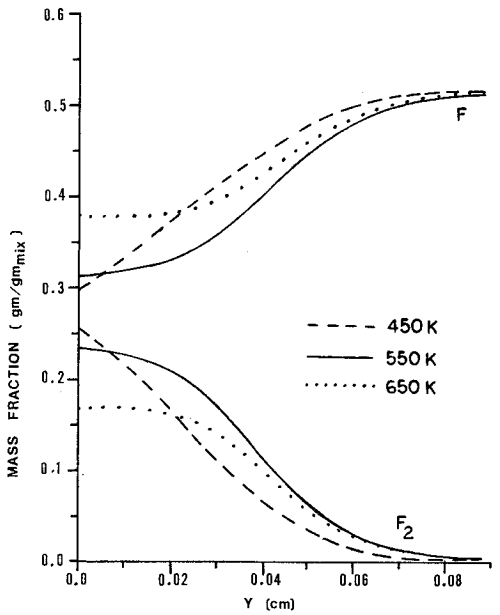

Fig. 6 Same as Fig. 4, but at exit plane.

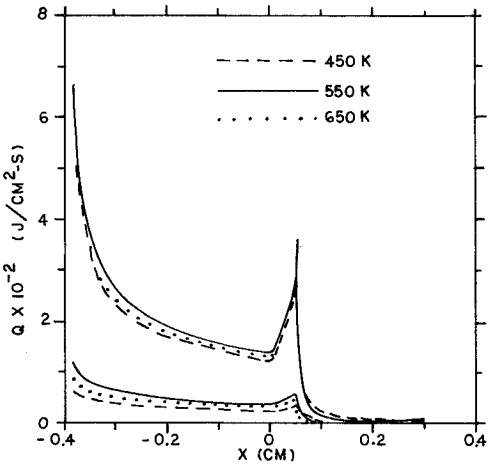

Fig. 8 Heat transfer to the wall for wall temperatures of 450, 550, 650 K. The lower curves are those portions due only to recombination predicted by the model of Ref. 2. The upper curves include both the heat transfer due to the temperature gradient at the wall and the recombination.

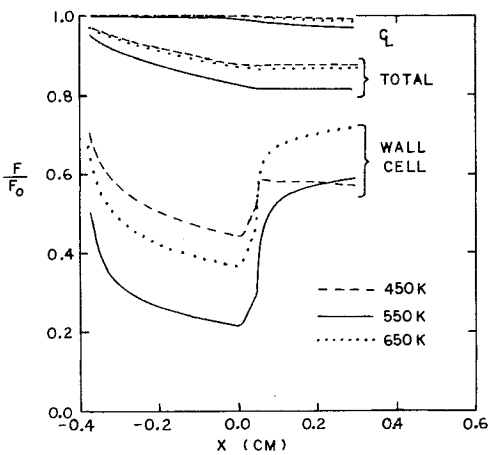

Fig. 7 Fraction of the fluorine depleted from the flow as a function of axial position, using the model of Ref. 2, for wall temperatures of 450, 550, 650 K.

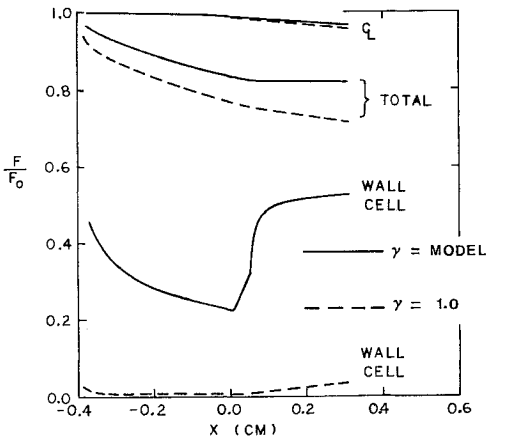

Fig. 9 Comparison of the depletion of atomic fluorine using the model of Ref. 2 and γ equal to 1.0 for a wall temperature of 500 K.

gradient-type heat transfer, the largest portion of which is in the subsonic section of the nozzle.

It is also possible to compare the use of a "real" recombination model to less rigorous models; in this regard, the model of Ref. 2 was run for a wall temperature of 500 K (the temperature found to give near maximum overall effect and compared to a fully catalytic wall where γ was assumed to be equal to one. In addition, the noncatalytic wall ($\gamma = 0.0$) was also run for a wall temperature of 500 K. The results are given in Figs. 9–13. A point that cannot be avoided is that the two wall-catalytic models yield large differences in the ultimate amount and distribution of species leaving the nozzle. Figure 9, for example, indicates that about 20% of the F is removed by the model of Ref. 2, whereas almost 30% is removed with $\gamma = 1.0$, a difference of half again, that is, a multiplier of 1.5. This difference does not seem nearly so great, however, when one realizes that the difference in γ's is approximately two orders of magnitude. The large difference in γ's and yet a much smaller difference in overall effect can be explained by realizing that the reaction is heavily diffusion-dependent in both cases.

The details in the species profiles predicted by the two catalytic wall models can be seen in Fig. 10. Also shown in Fig. 10 is the $\gamma = 0.0$ case, and it should be noted that there is a slight reduction in atomic fluorine at the wall along with an appropriate increase in molecular fluorine. This reflects the tendency of the fluorine to recombine at lower temperatures; however, the rate of gas-phase recombination is slow compared to the convection times, even near the wall. Thus, the flow is very nearly frozen. This leads to two conclusions: First, gas-phase reactions play a very minor role in these results; and second, the notion that the catalytic role of a wall is to simply expedite equilibrium chemistry because of the no-slip boundary condition is not justified. A final point concerning Fig. 10 is that for both models, the F concentration at the wall is not zero. This is true even when the wall is assumed to be fully catalytic. In fact, a $\gamma = 1.0$ is not physically realistic since at least for the steady-flow case, the maximum that γ can be is twice the steric factor, or 0.036. As noted in Refs. 2 and 7, γ could be higher than this during transients, but can never be larger than 1.0 (that is, by definition $\gamma \leq 1.0$). Thus, the assumption that fully catalytic

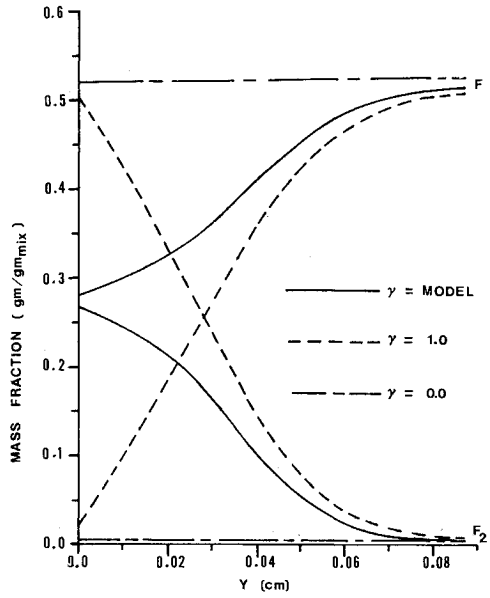

Fig. 10 Comparison of species profiles at the exit plane using a noncatalytic wall ($\gamma = 0.0$), a fully catalytic wall ($\gamma = 1.0$), and the model of Ref. 2, for a wall temperature of 500 K.

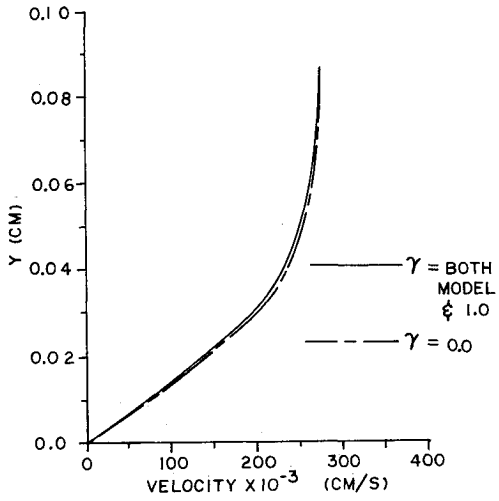

Fig. 11 Same as Fig. 10, but comparing velocity profiles.

may be interpreted as the concentration of F being zero at the wall is not, in general, a good one.

Figures 11 and 12 show how the wall-recombination models affect the velocity and temperature profiles, and it can be seen that the effect is not large. It can be seen from Fig. 13 that the heat transfer due to recombination is a major player in the subsonic section of the nozzle, and this also reflects only a small difference in magnitudes between models when compared to the large difference in magnitudes of the γ's.

VIII. Conclusions

This paper has attempted to demonstrate the effect of using a "realistic" wall-recombination model in predicting flow in the primary nozzle of a generic-type HF (or DF) laser. It can be seen that although differing from the results for a fully catalytic model, many of the essential features of the later-model results are preserved over a range in wall temperature from 450 to 650 K for the conditions and geometry analyzed here.

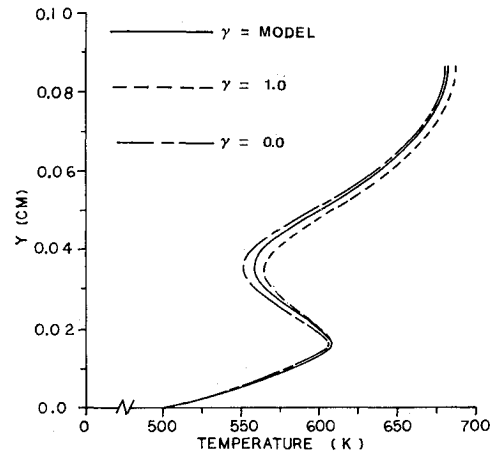

Fig. 12 Same as Fig. 10, but comparing temperature profiles.

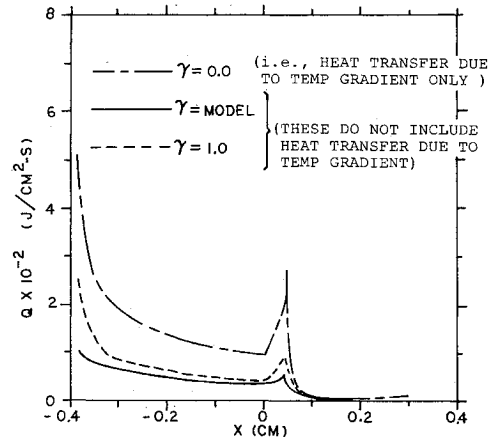

Fig. 13 Comparison of the heat transfer for the noncatalytic wall, the fully catalytic wall, and the model of Ref. 2. The top curve represents the heat transfer due to temperature gradient only and is common for all models, the lower curves show the additional heat transfer due to recombination, for a wall temperature of 500 K.

The effect of the subsonic section of the nozzle on the overall depletion of the atomic fluorine is clearly important. Although such subsonic sections are needed to provide passage for cooling ducts, a lesson to be learned is that they must be kept as short as possible.

Finally, a paper of this type seems long overdue, because the wall-recombination model discussed here has been available since 1980. The next obvious step is to repeat the calculations of Ref. 8 to see if the close match to experimental gain data is preserved using exit profiles like those in Fig. 6.

Acknowledgments

The authors wish to acknowledge the assistance of Dr. J. E. Hitchcock, Department of Aeronautics and Astronautics, Air Force Institute of Technology; and Dr. N. L. Rapagnani, Chief of Fluid Dynamics Branch, Air Force Weapons Laboratory.

References

[1]Gross, R. W. F. and Bott, J. F. (eds.), *Handbook of Chemical Lasers*, Wiley, New York, 1976.

[2]Jumper, E. J., Ultee, C. J., and Dorko, E. A., "A Model for Fluorine Atom Recombination on a Nickel Surface," *Journal of Physical Chemistry*, Vol. 84, January 1980, pp. 41-50.

[3]Rapagnani, N. L. and Davis, S. J., "Laser Induced I_2 Fluorescence Measurements in a Chemical Laser Flow Field," *AIAA Journal*, Vol. 17, 1979, pp. 1402–1404.

[4]Rapagnani, N. L., "The Effect of Heat Release in a Chemical Laser Cavity," *Proceedings 5th GCL Symposium*, Oxford Aug. 20–24, 1984, Institute of Physics Conference Series No. 72, Adam Hilger, Ltd: London, 1985, pp. 509–519.

[5]Spencer, D. J., "Sensitive F_2 Absorption Diagnostic," *Journal of Applied Physics*, Vol. 49, July 1978, pp. 3729–3732.

[6]Spencer, D. J., Durran, D. A., Bixler, H. A., and Varwig, R. L., "F_2 Boundary Layer Measurement in a Chemical Laser Slit Nozzle Flow," Air Force Systems Command, Space Division Rept. SD-TR-83-09, Los Angeles Air Force Station, CA, Feb. 1983 (AD A126611).

[7]Goldberg, I. B., "Measurements of Fluorine-Atom Recombination of a Nickel Surface by Electron Paramagnetic Resonance," *Journal of Physical Chemistry*, Vol. 84, November 1980, pp. 3199–3207.

[8]Mikatarian, R. R., Kurzius, S. C., McDanal, A. J., and Thoenes, J., "Analysis of Chemical Lasers, Vol. 2: Chemical Laser Analysis," TR-RK-CR-74-13, Propulsion Directorate, U.S. Army Missle Reserach, Development and Engineering Lab., Redstone Arsenal, June 1974.

[9]Ferrell, J. E., Kendall, R. M., and Tong, H., "Recombination Effects in Chemical Laser Nozzles," AIAA Paper 73-643, AIAA 6th Fluid and Plasma Dynamics Conference, July 1973.

[10]Langmuir, I., *Transactions of the Faraday Society*, Vol. 17, May 1922, p. 621.

[11]Rideal, E. K., *Proceedings of Cambridge Philosophical Society*, Vol. 35, 1939, p. 130; and *Chemistry and Industry*, (London), Vol 62, 1943, p. 335.

[12]Laidler, K. J., *Chemical Kinetics*, 2nd ed., McGraw-Hill, New York, 1965, Chap. 6.

[13]Emmett, P. H., *Catalysis, Vol. 1, Fundamental Principles*, Part I, Reinhold, New York, 1954.

[14]Glasstone, S., Laidler, J. J., and Eyring, H., *Theory of Rate Processes*, McGraw-Hill, New York, 1941.

[15]Vincenti, W. G. and Kruger, C. H. Jr., *Introduction to Physical Gas Dynamics*, Wiley, New York, 1967.

[16]Arutyunov, V. S. and Chaikin, A. M., *Kinetika I. Kalaliz*, Vol. 18, 1977, p. 321.

[17]Nordine, P. C. and Legrange, J. D., *AIAA Journal*, Vol. 14, 1976, p. 644.

[18]"JANAF Thermochemical Tables," The Dow Chemical Company, Midland, MI, 1963.

[19]Schlichting, H., *Boundary-Layer Theory*, 6th ed., McGraw-Hill, New York, 1968.

[20]Kays, W. M. and Crawford, M. E., *Convective Heat and Mass Transfer*, 2nd ed., McGraw-Hill, New York, 1980.

[21]Bronfin, B. R., "Development of Chemical Laser Computer Models," AFWL-TR-73-48, Air Force Weapons Lab., Kirtland, AFB, NM, July 1973.

[22]Bird, R. B., Stewart, W. E., and Lightfoot, E. N., *Transport Phenomena*, Wiley, New York, 1960.

[23]Jumper, E. J., Wilkins, R. G., and Preppernau, B. L., "Adaptation of a Wall-Catalytic Fluorine Recombination Model to Fluid-Dynamic Computations in an HF Laser Nozzle," AIAA Paper 85-1598, AIAA 18th Fluid Dynamics and Plasmadynamics and Laser Conference, July 16–18, 1985, Cincinnati, OH.